ELSEVIER

Mechanism of the interaction of Mn tetraazaporphines with peracetic acid
The comparative reactivity of Mn(III) porphinoid complexes in the formation of Mn-oxenes

Svetlana V. Barkanova[*], Elena A. Makarova

Organic Intermediates and Dyes Institute, B. Sadovaya 1/4, 103787 Moscow, Russia

Abstract

The mechanism of peracetic acid interaction with Mn(III) complexes of tetra-R-tetra-*tert*-butyl-tetraazaporphines (RTAPMnCl, R = H, Br, PhSO$_2$, NO$_2$) in acetonotrile/acetic acid solutions has been studied. Analysis of the kinetic data of *trans*-stilbene epoxidation, naphthalene hydroxylation, 1,1-diphenyl-2-picrylhydrazine (DPPH), and tetra-4-*tert*-butyl-phthalocyanine zinc (PcZn) one-electron oxidations revealed the reversible formation of a two-center molecular "catalyst–oxidant" complex ligated with a molecule of acetic acid {**A** = [RTAPMn(AcOOH)(AcOH)](X)}. The subsequent irreversible transformation of **A** with rate constant k_2 leads to the formation of two high-valent oxometallo species, supposedly [RTAPMn(V)(O)(AcOH)](X) and [$^{•+}$RTAPMn(IV)(O)(AcOH)](X), which are in equilibrium and show distinct oxidation abilities towards olefin and naphthalene. The Hammett-type dependencies of k_2 and of the rate constant of **A** formation (k_1) have been analyzed and compared with those ones determined earlier for Mn(III) meso-tetra(2,6-dichloro-4-R-phenyl)porphyrins (RTDCPPMnCl). The enhanced sensibility of the acceptor properties of Mn ion to electronegative substitution in tetraazaporphine macrocycle is considered to be a reason of the highest catalytic oxidative activity of Mn-tetra-nitro-tetra-*tert*-butyltetraazaporphine within studied Mn porphinoids. © 2001 Elsevier Science B.V. All rights reserved.

Keywords: Manganese tetraazaporphines; Peracetic acid; Oxidation; Mechanism

1. Introduction

Last 20 years cytochrome P-450 modeling with the employment of synthetic metalloporphyrins, mostly of iron and manganese complexes (PorM, M = Mn(III), Fe), have been widely studied [1–5]. Now it is commonly accepted that oxygen atom transfer from the oxidant (hydrogen peroxide [6], hydroperoxides [7,8], iodosylarenes [9], peracids [10–12], sodium hypochlorite [13,14], potassium monopersulfate ([15] and the references therein), amine N-oxides [16] and others) to the substrate (alkenes [1], alkanes [1,2], aromatics [15,17]) is fulfilled by reactive high-valent oxo-complexes, M(IV)-oxo-porphyrin π-cation radical and M(V)-oxo-porphyrin ([$^{•+}$PorM(IV)(O)](X) and [PorM(V)(O)](X), M = Fe, Mn). The reactivity of these moieties in the oxidation reactions significantly depends on the catalyst nature and on the structure of organic substrate as well. Thus, in olefins epoxidation catalyzed by Mn porphyrins, a species

[*] Corresponding author. Tel.: +7-95-2548877;
fax: +7-95-2541200.
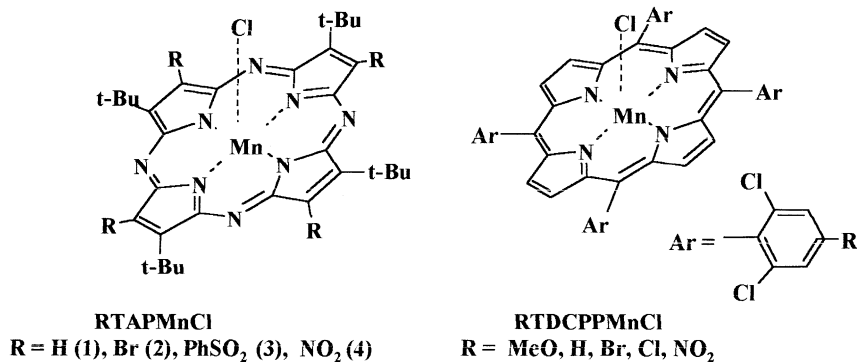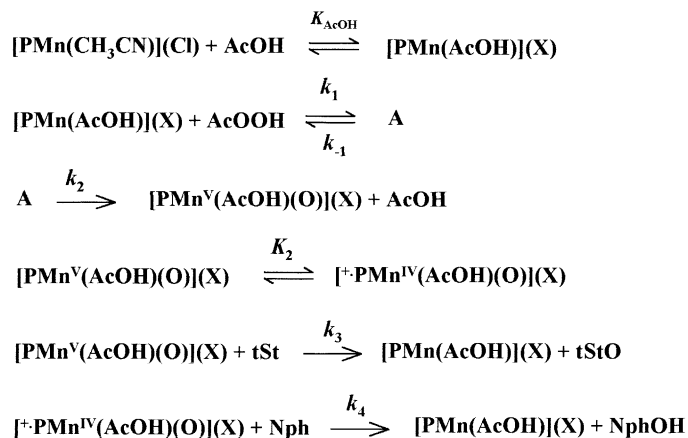*E-mail address:* rmeluk@cityline.ru (S.V. Barkanova).

Fig. 1. The structure of Mn(III) RTAPMnCl and Mn(III) RTDCPPMnCl.

of [PorMn(V)(O)](X)-type have been shown to be an oxygen-transferring agent to the double bond of olefin, producing *cis*-epoxide from the corresponding olefin with very high stereospecificity [4]. In the same reaction catalyzed by Fe porphyrins, both types of high-valent oxo-complexes $[^{\bullet+}PorFe(IV)(O)](X)$ and [PorFe(V)(O)](X) can produce epoxide [5]. On the other hand, the importance of the porphyrin 'hole' for affecting hydroxylation of organic substrates has been theoretically founded for the active forms of cytochrome P-450 and horseradish peroxidase [HRP(I)], where Fe(IV) ion is complexed with porphyrin π-cation radical [18]. It seems that in the case of Fe porphyrins $[^{\bullet+}PorFe(IV)(O)](X)$-type species possess both hydroxylation and epoxidizing properties. It should be mentioned that the nature and the reactivity of porphine-like Fe-oxo-complexes depend strongly on the macrocycle structure, in particular on meso-aza substitution. Thus, Fe complexes of azapoprphine derivatives (phthalocyanines, tetraazaporphines; APFe), effective catalysts of aromatics [15,17,19] and alkane [20] oxidation, are completely inactive in the reaction of olefin epoxidation by both peracetic acid [17] and KHSO$_5$ [21]. The activity of iron tetrasulfonatophthalocyanine in aromatics oxidation by KHSO$_5$ has been referred to the participation of $[^{\bullet+}APFe(IV)(O)](X)$-type species [15], inactive in olefin epoxidation [21]. Thus, the formation of the epoxidizing [APFe(V)(O)](X)-type moiety seems to be unlikely for aza analogs of Fe porphyrins.

So far, to our knowledge, there are only few data about comparative study of the reactivity of high-valent oxo-species for manganese complexes of

both porphyrins and azaporphines. Recently [22], we have came to the conclusion about distinct oxidation ability towards the substrates of two porphyrin Mn-oxo-complexes formed in the reaction of Mn(III) meso-tetraarylporphyrins with peracetic acid, one of which epoxidizes olefins and another one hydroxylizes aromatics to naphthols both in competitive and separate variants of oxidation procedures.

In our previous study, we have found that both Mn porphyrins (RTDCPPMnCl, R = H, NO$_2$) and their aza analogs (APMnCl, AP: octa-3,5-nitrophthalocyanine, tetra-*tert*-butyl-tetraazaporphine (**1**, Fig. 1)) efficiently catalyze olefins epoxidation by peracetic acid [23,24], whereas in the oxidation of non-activated aromatics to *p*-quinones nitro-substituted Mn azaphines are much more reactive than their porphyrin analog [17,19]. In order to understand the influence of meso-N substitution in the macrocycle on the oxidative reactivity of Mn porphine-like complexes, we have now studied the kinetics of substituted Mn(III) tetra-R-tetra-*tert*-butyl-tetraazaporphines (RTAPMnCl) (Fig. 1) interaction with peracetic acid using the approach developed earlier for Mn porphyrins [22]. This approach includes the kinetic study of four catalytic reactions carried out in acetonitrile/acetic acid solution: (1) olefin epoxidation to the corresponding epoxide; (2) naphthalene hydroxylation to 1-naphthol; (3) 1,1-diphenyl-2-picrylhydrazine (DPPH) one-electron oxidation to the corresponding stable radical (DPP$^{\bullet}$); (4) tetra-4-*tert*-butyl-phthalocyanine zinc (PcZn) one-electron oxidation to the stable π-cation radical ($^{\bullet+}$PcZn). The investigations of peracetic acid (AcOOH) interaction with Mn(III)

$$[PMn(CH_3CN)](Cl) + AcOH \xrightleftharpoons{K_{AcOH}} [PMn(AcOH)](X)$$

$$[PMn(AcOH)](X) + AcOOH \xrightleftharpoons[k_{-1}]{k_1} A$$

$$A \xrightarrow{k_2} [PMn^V(AcOH)(O)](X) + AcOH$$

$$[PMn^V(AcOH)(O)](X) \xrightleftharpoons{K_2} [^{\bullet+}PMn^{IV}(AcOH)(O)](X)$$

$$[PMn^V(AcOH)(O)](X) + tSt \xrightarrow{k_3} [PMn(AcOH)](X) + tStO$$

$$[^{\bullet+}PMn^{IV}(AcOH)(O)](X) + Nph \xrightarrow{k_4} [PMn(AcOH)](X) + NphOH$$

Scheme 1.

meso-tetra(2,6-dichloro-4-R-phenyl)porphyrins (RT-DCPPMnCl, R = MeO, H, Br, Cl, NO$_2$; Fig. 1) revealed that this reaction begins from the reversible formation of a two-center donor–acceptor complex of "catalyst–oxidant"-type ligated with a molecule of acetic acid {A = [RTDCPPMn(AcOOH)(AcOH)](X)}, which further undergoes irreversible transformation to the equilibrium mixture of Mn-oxo-complexes, [RTDCPPMn(V)(O)(AcOH)](X) and supposedly [$^{\bullet+}$RTDCPPMn(IV)(O)(AcOH)](X) (Scheme 1, P = porphyrin macrocycle). The *cis*-stilbene and naphthalene were shown to be effective traps of Mn-oxo-species [RTDCPPMn(V)(O)(AcOH)](X) and [$^{\bullet+}$RTDCPPMn(IV)(O)(AcOH)](X)], respectively; DPPH and PcZn were used as the scavengers of the first reaction intermediate **A**. The elementary rate constants of **A** formation (k_1) and of its further transformation to porphyrin Mn-oxo-complexes (k_2) have been estimated and their Hammett-type dependencies have been analyzed [22]. The main goal of the investigations reported here is to establish similar structure/activity relationships for Mn(III) tetraazaporphines and to compare them with those ones for Mn(III) porphyrins.

2. Experimental

2.1. Instrumentation

GC analyses were performed on a GC chromatograph "Tsvet-100" equipped with computing integrator C1-100 (glass column, Apiezon L 2 m, $T_{col} = T_{inj} = 200°C$, or OV 225, 2 and 0.5 m, $T_{col} = 130°C$, $T_{inj} = 150°C$, FID, He was used as a carrier gas). High performance liquid chromatography analyses were fulfilled on chromatograph "Milichrom-1A" supplied with computing integrator C1-100 and UV detector (Silosorb C$_{18}$ reverse-phase column; mobile phase: (a) gradient 0–100% CH$_3$CN in aqueous 0.01 M KH$_2$PO$_4$ adjusted to pH 3 with H$_3$PO$_4$, or (b) 10–100% aqueous CH$_3$CN. $\lambda_{anal} = 230$ and 280 nm for 1-naphthol and naphthalene, respectively). Reaction products were identified by coinjection of the reaction solution with the authentic samples onto HPLC or GC columns. Substrate and products quantitations were performed using standard plots of the authentic samples. Visible spectra were recorded with a fiber-optic spectrometer "LESA-7 Biospec".

2.2. Materials

Naphthalene, *trans*-stilbene and DPPH were commercial products and used as received. 1,1-Diphenyl-2-picrylhydrazyl (DPP) was obtained by DPPH oxidation with CrO$_3$ and reprecipitated two to three times with octane from benzene solutions. Acetonitrile (HPLC grade) was additionally purified by 1 month storage with potassium permanganate at room temperature, distillation under vacuum at 50–70°C, then treatment 24 h by CaCl$_2$ and 24 h by BaO or Ba(OH)$_2$. Solutions of peracetic acid

in acetic acid (1.3–1.9 M) were prepared as previously reported [23]. Freshly prepared reagent solutions in acetonitrile were employed in all experiments.

2.3. Catalysts

Tetra-R-tetra-*tert*-butyl-tetraazaporpine Mn(III) chlorides (**1**, **2**, **4**) were synthesized following reported procedure [17,24]. The free-base tetra-phenylsulfonyl-tetra-*tert*-butylporphyrazine (**3a**) was synthesized from tetra-bromo-tetra-*tert*-butylporphyrazine [25] by nucleophilic substitution of bromine atoms with sodium phenylsulfinate. Tetra-bromo-tetra-*tert*-butyl-porphyrazine (100 mg, 0.12 mmol) was refluxed 10 min in DMF (20 cm^3); after cooling (70°C), a solution of NaSO$_2$Ph·2H$_2$O (400 mg, 2.0 mmol) in DMF (5 cm^3) was added and stirred for 10 min. The reaction mixture was poured into ice–water (50 cm^3), the residue was filtered, washed with water (3 × 25 cm^3) and dried under vacuum. Column chromatography on silica gel with chloroform afforded a minor amount of the starting stuff; further elution with a mixture of chloroform:ethyl acetate (10:1) afforded **3a** (120 mg, 93%); R_f 0.77 (Silu-fol, chloroform:ethyl acetate = 10:1); λ_{max} (CHCl$_3$) (nm) (ε in dm^3 mol^{-1} cm^{-1}): 647 (7.08 × 10^4), 598 (6.20 × 10^4), 340 (6.77 × 10^4); m/z 1098 (M^+, 100%) for C$_{56}$H$_{58}$N$_8$O$_8$S$_4$; Anal. Calcd. for C$_{56}$H$_{58}$N$_8$O$_8$S$_4$: C, 61.18; H, 5.32; N, 10.19. Found: C, 61.68; H, 5.56; N, 9.62. Mn complex **3** was prepared as follows: a solution of **3a** (60 mg, 0.055 mmol) in DMSO (20 cm^3) was stirred for 15 min at room temperature with Mn(OAc)$_2$·4H$_2$O (67 mg, 0.27 mmol); the reaction mixture was poured into water (50 cm^3), the residue was filtered, washed with water (2 × 15 cm^3), 5% HCl (2 × 15 cm^3) and dried at ambient conditions. Two fractions were isolated by column chromatography on silica-gel with CHCl$_3$:acetone (10:1); the second one (R_f 0.24; silufol, chloroform:acetone = 10:1) was identified as **3** (24 mg, 42%); λ_{max} (CHCl$_3$) (nm) 650 (ε in dm^3 mol^{-1} cm^{-1}: 3.20 × 10^4); m/z 1151 (M^+, 100%) for [C$_{56}$H$_{56}$N$_8$O$_8$S$_4$Mn]$^+$. The first fraction is supposedly a mixture of 3- and 2-substituted Mn complexes (m/z 1014 (M^+) and 873 (M^+) for [C$_{50}$H$_{52}$N$_8$O$_6$S$_3$Mn]$^+$ and [C$_{44}$H$_{48}$N$_8$O$_4$S$_2$Mn]$^+$, respectively).

2.4. General method for trans-stilbene epoxidation

The mother solutions of *t*-St, RTAPMnX, and AcOOH in CH$_3$CN were prepared with concentrations three times those desired in reaction mixture. As an example, the procedure for *trans*-stilbene oxidation by **4** + AcOOH is reported. Acetonitrile solutions of [*t*-St]$_{in}$ = 0.03 M (1 ml) and of [**4**]$_{in}$ = 6 × 10^{-7} M (1 ml) were poured in a Schlenk tube, then 1 ml of 0.15 M solution of [AcOOH]$_{in}$ (1.31 M AcOOH in AcOH diluted 8.75 times with CH$_3$CN) was added and the mixture was kept under stirring. In the case of the reaction carried out at [AcOH]$_0$ = constant initial AcOOH solution in CH$_3$CN was prepared with the desired amount of AcOH (the AcOH concentration injected with the oxidant is marked as [AcOH]$_{ox}$). Samples of 0.2 ml were withdrawn at fixed time, the excess of AcOOH was quenched with KJ or tetra-butylammonium iodide and the mixture was analyzed by GC (OV 225 0.5 m column). In the case of KI employment, the upper part of GC glass column was cleaned with wet cotton after every 20 injections. For complexes **2**, **4** and **1** (at [**1**]$_0$ ≤ 10^{-6} M) kinetic curves of *trans*-stilbene disappearance and epoxide formation follow zero-order law up to 50–70% substrate conversion, and the rates of *trans*-stilbene disappearance W_{ol}^{obs} (equal to the rate of epoxide formation W_{ep}^{obs}) were calculated for the "initial" parts of kinetic curves. At 0.06–0.6 M [AcOH]$_0$, the reaction rates occur to be independent on acetic acid concentration. For all Mn complexes, the independence of $W_{ol(ep)}^{obs}$ on olefin concentration was observed at [*t*-St]$_0$ ≥ 0.005 M. The values of k_{ol} were determined as $W_{ol(ep)}^{obs}$/[catalyst]$_0$ at [AcOOH]$_0$ ≥ 0.025 M for **1** and **2** and ≥0.015 M for **4**, when the reaction rates exhibit independence on oxidant concentration. For complex **3**, k_{ol} value was calculated from the dependence $W_{ol(ep)}^{obs}$ on [AcOOH]$_0$ linearized in the coordinates (1/$W_{ol(ep)}^{obs}$) − (1/[AcOOH]$_0$).

2.5. General method for naphthalene hydroxylation

The kinetic measurements were carried out as described for *trans*-stilbene epoxidation; naphthalene disappearance was measured by GC (OV 225 2 m column), quenching the AcOOH excess with KJ. The concentration of formed 1-naphthol was measured by HPLC without AcOOH excess quenching;

at fixed time 5–10 μl of the reaction mixture was injected directly into HPLC column. The independence of W_{NphOH}^{in} on naphthalene concentration was observed at $[Nph]_0 \geq 0.004$ or 0.012 M for **1** and **3**, **4**, respectively. For low concentrations of complex **1** ($<10^{-5}$ M), kinetic curves of naphthalene disappearance obey zero-order law up to no more than 50% substrate conversion through catalyst destruction. The rate of naphthalene disappearance (W_{Nph}^{in}) determined for this "initial" part of the kinetic curve is equal to the initial rate of 1-naphthol formation, thus evidencing that 1-naphthol is a single primary product of naphthalene oxidation. The value of k_{Nph} for complex **1** was calculated as follows: the dependence of W_{Nph}^{in} on the AcOOH concentration was plotted in the reciprocal coordinates ($(1/W_{Nph}^{in}) - (1/[AcOOH]_0)$); the y intercept of this plot provides $1/(k_{Nph} \times [\mathbf{1}]_0)$. We were induced to use very low catalysts concentrations of high reactive complexes **3** and **4** (10^{-7} to 10^{-8} M) to make the reaction rates measurable, and due to the catalyst deficiency (destruction) the conversion of naphthalene was very low; thus, the comparison of W_{NphOH}^{in} with W_{Nph}^{in} for **3** and **4** was not accomplished. For catalyst **3**, exhibiting high propensity to the side radical decomposition of an oxidant, the kinetic curves of 1-naphthol formation were measured at low $[AcOOH]_0 = 0.001–0.003$ M, and k_{NphOH} value was evaluated from Eq. (1) using K_1 value, established in *trans*-stilbene oxidation. We failed to estimate k_{NpfOH} for complex **2** through its elevated reactivity in further 1-naphthol oxidation.

2.6. The trans-stilbene oxidation in the presence of 1,1-diphenyl-2-picrylhydrazyl (DPP•) and complex 3

The mother solutions of *trans*-stilbene, DPP•, **3** and AcOOH in acetonitrile were prepared with concentrations four times those desired in reaction mixture. The experiments were carried out as described for *trans*-stilbene. The concentrations of *trans*-stilbene and *trans*-stilbene epoxide were measured by GC with AcOOH quenching by KJ.

2.7. 1,1-Diphenyl-2-picrylhydrazyn and Zn-tetra-tert-butyl-phthalocyanine (PcZn) oxidation

General methods of DPPH and PcZn oxidations are described in [22]. At any used $[AcOH]_0$, both

substrates are oxidized without spectral changes of Mn tetraazaporphines to DPP• and to •⁺PcZn with maximal DPP• yield or PcZn conversion up to 100% ($\eta_{DPP•} = 2[DPP•]_{max}/[AcOOH]_0$). The stoichiometry of the reaction calculated as $[DPP•]_{maximal}/[AcOOH]_0$ or $[PcZn]_{reacted}/[AcOOH]_0$ was found near to 2:1. The values of bimolecular rate constant of DPP• formation and of PcZn bleaching k_g^{obs} and k_{Pc}^{obs} were calculated from the equation $k_{g(Pc)}^{obs} = W_{DPP(Pc)}/(2[RTAPMnCl]_0 \times [AcOOH]_0)$. The values of k_g^{obs} and k_{Pc}^{obs} determined at the reaction rate independence of $[AcOH]_0$ are given as k_g and k_{Pc}, respectively. The values of equilibrium constant of **A** dissociation (K_d) for catalysts **2** and **4** were calculated from the equation $K_d = (K[AcOH]_0)^{1/2}/(\tan \alpha \times k_1)$; the calculation of $\tan \alpha$ is evident from Fig. 8b; the dissociation constant of acetic acid in acetonitrile K was assumed equal to 2.5×10^{-12} M [26].

3. Results and discussion

3.1. Kinetics of trans-stilbene epoxidation and naphthalene hydroxylation

Earlier it has been shown [24] that in contrary to sterically hindered Mn meso-tetraarylporphyrins, Mn azaporphines catalyze the epoxidation of both *cis*- and *trans*-olefins quantitatively and stereospecifically, the reaction rates being independent on the olefin structure. Hence, in this study *trans*-stilbene was used as a trap of Mn(V)-oxo-moiety. Catalytic epoxidation of *trans*-stilbene to *trans*-stilbene epoxide and naphthalene hydroxylation to 1-naphthol were carried out with peracetic acid solutions in acetic acid at the reagent concentrations reported in Table 1. The determinations of the reaction rates of *trans*-stilbene and naphthalene disappearance of *trans*-stilbene epoxide and 1-naphthol formations so as the method of the observed rate constant values calculations are described in Section 2.

Similar to Mn porphyrins, both the rate of olefin disappearance (W_{ol}^{obs}) and the initial rate of 1-naphthol formation [1] (W_{NphOH}^{in}) were determined in such a re-

---

[1] The intimate mechanism of oxygen atom transfer from oxene **6** to the molecule of naphthalene is now under study and will be discussed later.

Table 1
The *trans*-stilbene and naphthalene oxidation with peracetic acid catalyzed by RTAPMnCl ($CH_3CN + AcOH$, 20°C)[a]

$[RTAPMnCl]_0$ (M)[b]	$[t$-St$]_0$ (M)[b]	$[Nph]_0$ (M)[b]	$[AcOOH]_0$ (M)[b,c]	K_1 (dm^3 mol^{-1})	k_{ol} (s^{-1})	k_{Nph} (s^{-1})
1: (0.8–10) × 10^{-6}	0.005–0.01	0.002–0.008	0.005–0.06	50[d]; 45[e]	3.0	1.4
2: (0.51–5.0) × 10^{-6}	0.005–0.02	–	0.01–0.05	40	3.2	–
3: (0.02–3.3) × 10^{-6}	0.005–0.01	0.012–0.025	0.005–0.05[d]; 0.001–0.01[e]	30	140	∼80[f]
4: (0.5–2.0) × 10^{-7}	0.01	0.004–0.025	0.005–0.05	120	1070	550

[a] Reagent concentrations, K_1, k_{ol} (k_2), k_{Nph}, and K_2 values.

[b] Several measurements were done within shown concentration intervals; experimental errors in the rate constant values determination and in K_1 estimation are 20% (±10) and 50% (±25) relative, respectively.

[c] Reaction solutions contain acetic acid injected with "mother" solution of AcOOH ($[AcOH]_{ox} \cong 10[AcOOH]_0$); some experiments (Fig. 2a) were done at $[AcOH]_0 = const = [AcOH]_{ox} + [AcOH]_{added}$; calculated for **1**, **2**, and **4**, k_{ol}, k_{ep}, and K_1 values were found to be independent of acetic acid concentration at $[AcOH]_0 \geq 0.06$ M; all experiments were done for $[RTAPMn(III)(AcOH)](X)$ coordination state.

[d] Determined in *trans*-stilbene epoxidation.

[e] Determined in naphthalene hydroxylation.

[f] Calculated from equation $k_{Nph} = W_{NphOH}/\{K_1[3]_0 \times [AcOOH]_0\}$ with accuracy ±40%.

gion of substrate concentration, where the reaction rates are independent on the last, i.e. when olefin and naphthalene act as traps of high-valent catalyst species. Both of them are first order in $[RTAPMnCl]_0$ and exhibit Michaelis–Menten-type dependence on $[AcOOH]_0$ (Figs. 2–4, Eq. (1)).

$$W_{ol(NphOH)} = \frac{k_{ol(Nph)} K_1 [RTAPMnX]_0 [AcOOH]_0}{1 + K_1 [AcOOH]_0} \tag{1}$$

$$W_{ol(NphOH)} = k_{ol(Nph)} [RTAPMnX]_0,$$
$$\text{at } K_1 [AcOOH]_0 > 1 \tag{1a}$$

It is worth noting that at the elevated oxidant concentration ($[AcOOH]_0 > 0.05$ M for **1**, **2** and **4** or >0.025 M for **3**), the epoxide yield determined at every point of the reaction as $[epoxide]_{formed}/[olefin]_{reacted}$ is less than 100%. In the case of Mn porphyrins, similar effect was explained by possible competitive radical decomposition of peracid excess followed by non-selective olefin oxidation [24]. To clarify whether this hypothesis comes true for Mn tetraazaporphines, we have employed stable radical 1,1-diphenyl-2-picrylhydrazyl (DPP•) as a trap[2] of AcO• and AcO$_2$•, presumably efficiently

---

[2] Well-known radical traps (e.g. 2,6-di-*tert*-butylphenol) cannot be used in the reactions catalyzed by Mn azaporphines because of their oxidation to *p*-quinones, e.g. in the presence of APMnX 2,3,6-trimethylphenol-1 is quickly and quantitatively converted to 2,3,6-trimethyl-1,4-benzoquinone at two times AcOOH excess.

formed in the side-oxidant decomposition during the *trans*-stilbene epoxidation catalyzed by complex **3**. In a good agreement with the supposition, in the presence of DPP•, the *trans*-stilbene epoxide yield becomes quantitative at every point of the reaction (Fig. 5). Moreover, in this case the maximal olefin conversion increases, apparently due to the catalyst protection from oxidative degradation by AcO• and/or AcO$_2$•, which in turn leads to the enhanced catalyst turnover number (TN = [substrate]$_{reacted}$/[catalyst]$_0$).

The values of monomolecular rate constants k_{ol} and k_{NpfOH} were calculated from Eq. (1a) for such a region of $[AcOOH]_0$, where the reaction rates are independent on the oxidant concentration. For complexes **1**, **3** and **4**, k_{NpfOH} values occur to be two times less than that of k_{ol} (Table 1). Furthermore, the value of the equilibrium constant K_1 calculated in naphthalene hydroxylation using Eq. (1) and data reported in Fig. 6 is similar to one determined in *trans*-stilbene epoxidation (Table 1), indicating the formation of the same first intermediate **A** in both reactions. The reported data are similar to those observed earlier [22] for Mn tetraarylporphyrins (Table 2), thus evidencing that the reaction of peracetic acid interaction both with the porphyrin and tetraazaporphine Mn(III) complexes is described by one and the same reaction mechanism (Scheme 1). Calculated from Scheme 1, equations for epoxide and 1-naphthol formations in olefin and naphthalene oxidation are identical to the experimentally determined Eq. (1) at $k_{ol} = k_2$ and $k_{Nph} = k_2 K_2/(1 + K_2)$
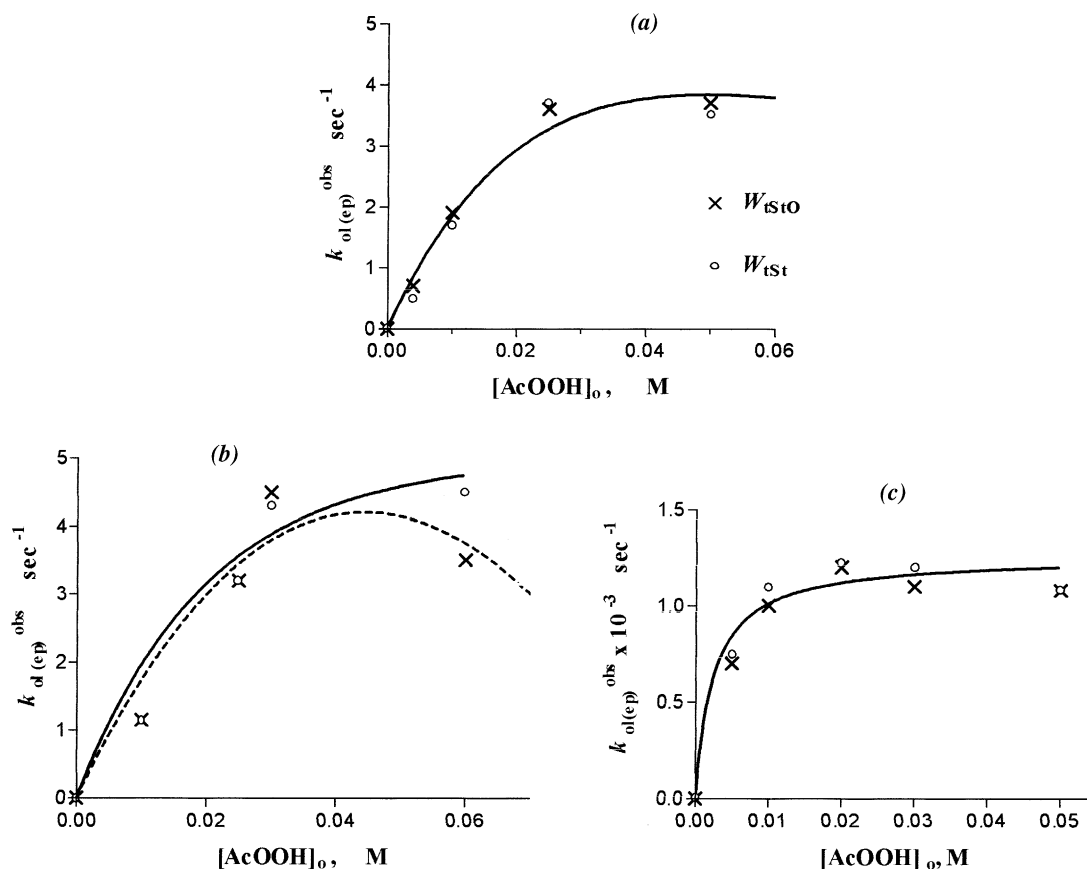
Fig. 2. The dependence of partial rates ($k_{ol(ep)}^{obs} = W_{ol(ep)}/[RTAPMnCl]_0$) of *trans*-stilbene disappearance and *trans*-stilbene epoxide formation on $[AcOOH]_0$ in the reaction catalyzed by **1**, **2**, and **4**: (a) $[\mathbf{1}]_0 = 1.6 \times 10^{-6}$ M, $[t\text{-St}]_0 = 0.005$ M, $[AcOH]_0 = 0.6$ M; (b) $[\mathbf{2}]_0 = 5 \times 10^{-6}$ M, $[t\text{-St}]_0 = (0.5–1) \times 10^{-2}$ M, $[AcOH]_{ox} = 0.1–0.6$ M; (c) $[\mathbf{4}]_0 = 1 \times 10^{-7}$ M, $[t\text{-St}]_0 = 0.01$ M, $[AcOH]_{ox} = 0.05–0.6$ M.

(Eqs. (2) and (3)):

$$k_{ol} = k_2 \tag{2}$$

$$k_{Nph} = \frac{k_2 K_2}{1 + K_2} \tag{3}$$

Thus, with this approach the value of the rate constant k_2, a criterion of RTAPMnCl reactivity in Mn(V)-oxo-complex formation, could be easily determined from the experiment as k_{ol} value.[3] Scheme 1 though disregards the possibility of **A** dissociation and Mn-oxo-species formation from peroxoacetates **A⁻**, whereas both variants of the reaction are feasible and

should be considered. Indeed, molecular complexes of PorFe and PorMnX with H_2O_2 [6], alkyl hydroperoxides [27,28] and amine N-oxides [16] were kinetically detected as primary intermediates; they were also suggested in PorMn interaction with NaOCl [29] and iodosylbenzene [30–32]. On the other hand, peracids interaction with Fe and Mn porphyrins was postulated to occur with 'persalts' (PorMOOCOR) formation as precursors of high-valent metalloxo-species [33–36]. If the last comes true in the reported catalytic systems, theoretically calculated equations for the rates of *trans*-stilbene and naphthalene oxidation would fit with experimentally determined Eq. (1) at k_{ol} and k_{Nph} expressed by Eqs. (4) and (5):

$$k_{ol} = k_2' K_d \tag{4}$$

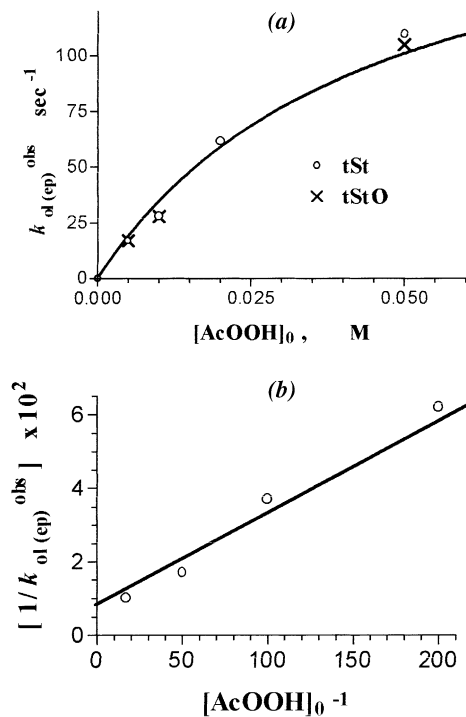[3] In [22], rate constant k_{ol} for Mn porphyrins was erroneously attributed as $k_2/(1 + K_2)$.

Fig. 3. (a) The dependence of partial rate of *trans*-stilbene disappearance (k_{ol}^{obs}) and *trans*-stilbene epoxide formation (k_{ep}^{obs}) on $[AcOOH]_0$ in the reaction catalyzed by **3**; (b) linearization of the dependence (a). $[\mathbf{3}]_0 = 3.3 \times 10^{-6}$ M, $[t\text{-St}]_0 = 0.005$–0.01 M, $[AcOH]_0 = 0.5$ M. At $[AcOOH]_0 = 0.05$ M, $k_{ol(ep)}^{obs}$ was determined in the presence of DPP$^\bullet$ (data from Fig. 5).
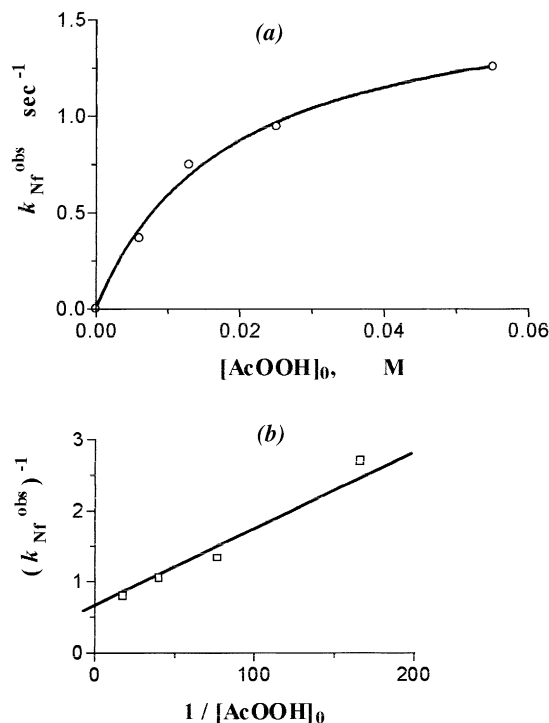

Fig. 4. (a) The dependence of partial rate ($k_{Nph}^{obs} = W_{Nph}/[RTAPMnCl]_0$) of naphthalene disappearance on $[AcOOH]_0$ in the reaction catalyzed by **1**; (b) linearization of the dependence (a). $[\mathbf{1}]_0 = 1 \times 10^{-5}$ M, $[Nph]_0 = 0.0025$ M, $[AcOH]_0 = 0.55$ M.
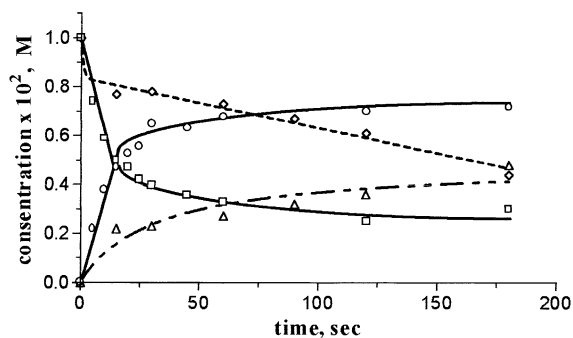
$$k_{Nph} = \frac{k_2' K_2 K_d}{1 + K_2}, \quad \text{at } 1 > K_d \tag{5}$$

where k_2' is the rate constant of $\mathbf{A}^-$ transformation to Mn(V)-oxo-complex.

To clarify this problem, we have used two different compounds, DPPH and PcZn as scavengers of the first intermediate **A** and have investigated the influence of acetic acid on the kinetics of their one-electron oxidation to the corresponding stable radical (DPP$^\bullet$) and stable π-cation radical ($^{\bullet+}$PcZn, $\lambda_{max} = 510$, 725 nm [37]), respectively. If the equilibrium $A \leftrightarrow A^- + H^+$ does exist, the rates of DPPH and PcZn oxidation should depend on acid addition, supposing that the oxidation activities of **A** and $\mathbf{A}^-$ are different.

Fig. 5. Kinetic curves of *trans*-stilbene disappearance ($\square$, $\diamondsuit$) and *trans*-stilbene epoxide formation ($\bigcirc$, $\triangle$) in *trans*-stilbene oxidation by peracetic acid catalyzed by **3** in the presence of 1,1-diphenyl-2-picrylhydrazyl ($[DPP^\bullet]_0 = 0.025$ M; $\square$, $\bigcirc$) and without hydrazyl ($\diamondsuit$, $\triangle$). $[\mathbf{3}]_0 = 3.3 \times 10^{-6}$ M, $[AcOOH]_0 = 0.05$ M, $[AcOH]_{ox} = 0.56$ M.
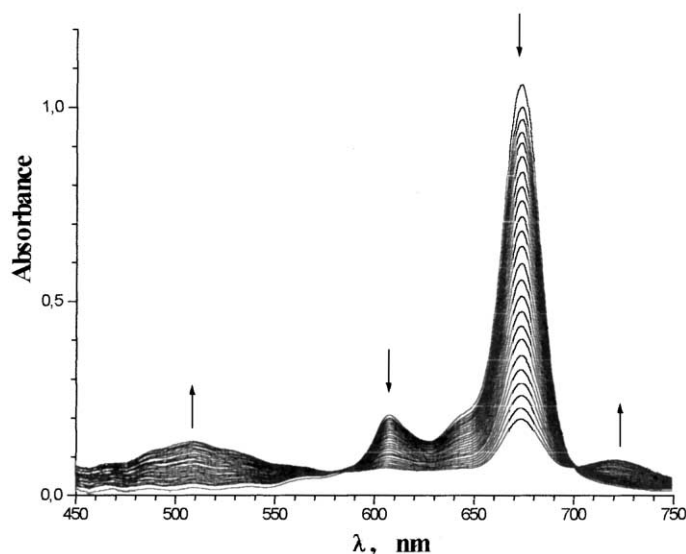
Fig. 6. Visible spectra changes in the reaction of PcZn oxidation by peracetic acid catalyzed by complex **1**. $[\mathbf{1}]_0 = 0.5 \times 10^{-7}$ M, $[PcZn]_0 = 3 \times 10^{-5}$ M ($\varepsilon_{674\,nm} = 2.2 \times 10^5$), $[AcOOH]_0 = 0.5 \times 10^{-4}$ M, $[AcOH]_0 = 0.2$ M, $l = 0.2$ cm, time intervals 30 s.

3.2. 1,1-Diphenyl-2-picrylhydrazine and Zn-tetra-tert-butyl-phthalocyanine oxidation: the influence of acetic acid

Previously, we have shown that UV–VIS spectra of Mn tetraazaporphines acetonitrile solutions (10^{-6} to 10^{-4} M) obey Lambert–Beer's law and do not change at 0.001–0.5 M acetic acid addition. The highest AcOH content was limited by the protonation of both DPPH and PcZn, noticeable at $[AcOH]_0 > 0.1$ and >0.5 M, respectively. The used concentrations of catalysts and substrates are indicated in Table 3.

For the reactions of DPPH oxidation as well as of PcZn discoloration (Fig. 6), we have measured the reaction rates of DPP• formation (W_{DPP}) or PcZn bleaching (W_{Pc}) at several concentrations of acetic acid. At every $[AcOH]_0$, the rate of DPP• formation so that the rate of PcZn bleaching was found to be first order both in $[AcOOH]_0$ and $[RTAPMnX]_0$ and independent on the substrate concentration at $[DPPH]_0 \geq 10^{-3}$ M in DPPH oxidation and at $[PcZn]_0 \geq 1 \times 10^{-5}$ M in PcZn oxidation. The kinetic curves of both reactions obey zero-order law up to 75% maximal concentration of formed DPP• and up to 90% PcZn conversion. Thus, the used substrates DPPH and PcZn act as real traps for the oxidative intermediate, i.e. the

first reaction stage in Scheme 1 becomes irreversible and the rates W_{DPP} (W_{Pc}) and **A** (or **A**$^-$) formation are equal taking into account the stoichiometric coefficient 2.

As it turned out, the rates of both reactions depend strongly on the concentration of added acetic acid (Figs. 7 and 8 exemplify the acidic dependencies for complexes **1** and **4**, respectively). The first phase of the observed acidic dependencies can

Table 2
The values of k_{ol} (k_2), k_{Nph}, and k_1 for acidic adducts of Mn(III) meso-tetra(2,6-dichloro-4-R-phenyl)porphyrins {[RTDCPPMn(AcOH)](X), X = Cl, AcO} determined in *cis*-stilbene, naphthalene, 1,1-diphenyl-2-picrylhydrazine, and Zn-tetra-4-*tert*-buthylphthalocyanine catalytic oxidation by peracetic acid[a]

$[RTDCPPMnCl]_0$	k_{ol} (s^{-1})	k_{Nph} (s^{-1})	k_1 $(dm^3\,mol^{-1}\,s^{-1})$
H	0.85	0.38	200
MeO	1.0	0.51	210
Br	1.8	0.94	260
Cl	2.0	0.85	220
NO$_2$	4.3	3.65	230

[a] CH$_3$CN + AcOH, 20°C; $[AcOH]_0$:$[RTDCPPMnCl]_0 \geq$ 1000:1 (from [22]).

Table 3
Reagent concentrations and k_1 values determined in the reactions of DPPH and PcZn oxidation by peracetic acid catalyzed by RTAPMnCl[a]

[RTAPMnCl]$_0$ (M)[b]	[DPPH]$_0$ (M)[b]	[PcZn]$_0$ $\times 10^5$ (M)[b]	[AcOOH]$_0$ $\times 10^5$ (M)[b]	[AcOH]$_0$ (M)[b]	k_1 (dm^3 mol^{-1} s^{-1})
1: $(0.5–1) \times 10^{-6}$ [c]; $(0.17–1) \times 10^{-7}$ [d]	$(1–2) \times 10^{-3}$	1.2–3.0	2.5–6.0[c]	0.001–0.1 [c]; 0.1–0.3 [d]	4.5×10^3 [c,e]; 5.0×10^3 [d]
2: $(0.1–1.0) \times 10^{-7}$		1.0–3.0	2.5–10.0	0.01–0.05	1.5×10^4 [d]
3: $(1.0–2.5) \times 10^{-7}$	$(1–2) \times 10^{-3}$		4.0	0.06–0.1	8.0×10^4 [c]
4: $(0.5–1.0) \times 10^{-9}$		1.0–3.0	5–10.0	0.02–0.06	2.7×10^5 [d]

[a] CH$_3$CN + AcOH, 20°C.

[b] Several measurements were done within shown concentration intervals; the rate of base-line DPPH oxidation by AcOOH (~10% from the catalytic one) was subtracted from the summary rate of DPP$^\bullet$ formation in the catalytic reaction; the rate of base-line PcZn oxidation by AcOOH was less than 2% from the catalytic one; the values of k_1 were calculated with accuracy 20% ($\pm$10) relative; for the reaction of PcZn oxidation within indicated [AcOH]$_0$, the rate of PcZn bleaching does not depend on [AcOH]$_0$.

[c] Calculated for [RTAPMn(AcOH)](X) in DPPH oxidation.

[d] Calculated for [RTAPMn(AcOH)](X) in PcZn oxidation.

[e] The value $k_1 = 48$ dm^3 mol^{-1} s^{-1} for **1** published earlier [24] was calculated for the mixture of [TAPMn(CH$_3$CN)](X) and [TAPMn(AcOH)](X) adducts.

be explained by the formation of acetic adduct [RTAPMn(AcOOH)(AcOH)](X) instead of acetonitrilic one, possessing the enhanced reactivity in DPPH and PcZn oxidations; in Mn tetraarylporphyrins study, we have came to the same conclusion [22]. Recently, the significant influence of axial ligand nature (acids, solvent molecules, etc.) on the oxidative properties of oxygen-containing intermediates has been reported for substituted metalloporphyrins [5,38]. The independence of W_{DPP} and W_{Pc} on the acetic acid content on the second phase of acidic dependencies (Figs. 7 and 8) evidences that in this [AcOH]$_0$ region, the
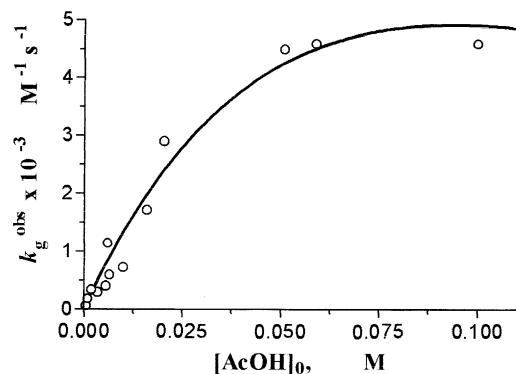

Fig. 7. The AcOH dependence of partial rate $\{k_g^{obs} = W_{DPP}/(2[\mathbf{1}]_0 \times [AcOOH]_0)\}$ of DPP$^\bullet$ formation in DPPH oxidation by peracetic acid catalyzed by complex **1**. [DPPH]$_0 = 2 \times 10^{-3}$ M, [**1**]$_0 = 1 \times 10^{-6}$ M, [AcOOH]$_0 = 0.5 \times 10^{-4}$ M.
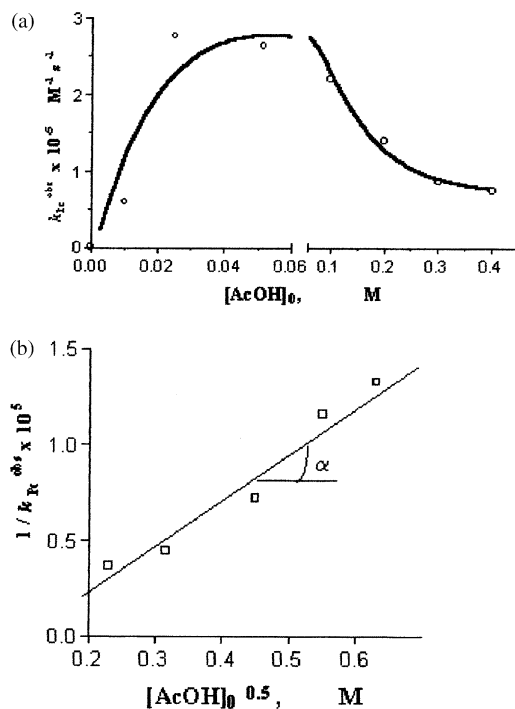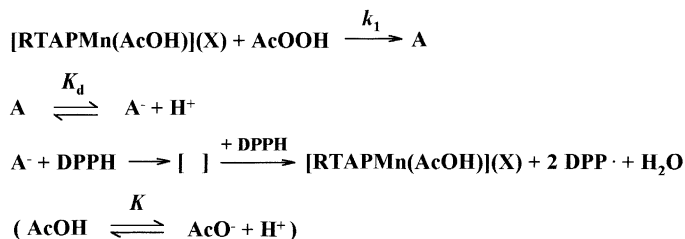

Fig. 8. (a) The dependence of partial rate of PcZn bleaching $\{k_{Pc}^{obs} = W_{Pc}/(2[\mathbf{4}]_0 \times [AcOOH]_0)\}$ on [AcOH]$_0$ for complex **4**; (b) linearization of the dependence (a) at [AcOH]$_0 = 0.06$–0.4 M. [**4**]$_0 = (0.3–1) \times 10^{-9}$ M, [AcOOH]$_0 = (0.5–1) \times 10^{-4}$ M, [PcZn]$_0 = (1–3) \times 10^{-5}$ M.

$$[RTAPMn(AcOH)](X) + AcOOH \xrightarrow{k_1} A$$

$$A \overset{K_d}{\rightleftharpoons} A^- + H^+$$

$$A^- + DPPH \longrightarrow [\quad] \xrightarrow{+ DPPH} [RTAPMn(AcOH)](X) + 2\,DPP\cdot + H_2O$$

$$(\,AcOH \overset{K}{\rightleftharpoons} AcO^- + H^+\,)$$

Scheme 2.

equilibrium between acetonitrilic and acidic catalyst adducts is fully shifted to the formation of acidic ones. In this case, bimolecular rate constant values of DPP$^\bullet$ formation or of PcZn bleaching (k_g and k_{Pc}) should be referred to the Mn tetraazaporphines acidic adducts [RTAPMn(AcOOH)(AcOH)](X). For complex **1**, the k_{Pc} value determined on the second phase of acidic dependence at $[PcZn]_0 \geq 1 \times 10^{-5}$ M is very close to k_g values obtained in DPPH oxidation at $[DPPH]_0 \geq 10^{-3}$ M (Table 3), thus evidencing that PcZn and DPPH trap one and the same catalytic intermediate.

The decrease of the reaction rate in the third phase of acidic dependencies for less basic PcZn points strongly that molecular complex **A** undergoes dissociation and that the reactivity of the formed peroxoacetate **A**$^-$ in one-electron oxidation is higher than that of **A**. Scheme 2 represents the simplest mechanism of DPPH (as well as PcZn) oxidation; theoretically calculated from Scheme 2, equations for the reaction rates of the third phase fit well with the experimental one at $k_{g(Pc)}$ expressed by Eq. (6).

$$
\begin{aligned}
k_{g(Pc)} &= \frac{W_{DPP(Pc)}}{2[RTAPMnX]_0[AcOOH]_0} \\
&= \frac{k_1 K_d}{(K[AcOH]_0)^{0.5} + K_d}
\end{aligned}
\tag{6}
$$

Satisfactory linearization of the third phase of acidic dependencies in the coordinates $(1/k_{Pc}^{obs}) - [AcOH]_0^{0.5}$ (Fig. 8b) is in a good agreement with the proposed Scheme 2 and Eq. (6). According to this equation, at the reaction rate independence of $[AcOH]_0$, i.e. at $K_d > (K[AcOH]_0)^{0.5}$, experimentally determined $k_{g(Pc)}$ values are equal to the elementary rate constant k_1 (Table 3). From Eq. (6), we have also estimated the values of K_d for molecular complexes **A** of catalysts **2**

and **4** ($\sim 0.6 \times 10^{-6}$ and $\sim 0.3 \times 10^{-6}$ M, respectively; the calculations are described in Section 2).

3.3. The nature of Mn-oxenes precursor: the comparison of the Mn tetraazaporphines and Mn tetraarylporphyrins reactivity in their interaction with peracetic acid

Although, the dissociation of molecular complex **A** under the reaction conditions seems to be proved, the exact nature of Mn-oxo-complexes precursor is still questioned. Really, if Mn-oxo-species are formed with the rate constant k_2' from peracetate **A**$^-$, unknown K_d value in Eqs. (4) and (5) and derived from them Eq. (7)

$$(\ln k_2')^{rel} = \ln \frac{(k_2')^R}{(k_2')^H} = \ln k_{ol}^{rel} - \ln \frac{K_d^R}{K_d^H} \tag{7}$$

complicates the k_2' calculation, hence, the establishing of catalyst structure/activity relationship. Nevertheless, slight changes in K_d values, together with the sharply expressed dependence of k_{ol} on the substituent nature (for **2** and **4** k_{ol} and K_d values differ 300 and 2 times, respectively) allow to disregard the second member in Eq. (7) as compared to the first one and consider $\ln (k_2')^{rel} = \ln k_{ol}^{rel}$. Hence, if Mn-oxo-moieties are produced from the dissociated form **A**$^-$, the experimentally determined relative rate constant $k_{ol} = k_{ol}^R/k_{ol}^H$ can be used as correct criterion of RTAPMnCl relative reactivity in the Mn(V)-oxo-complex formation.

For Mn tetraazaporphines, non-linear correlation of $\ln k_{ol}^{rel}$ in the coordinates of Hammett equation (Fig. 9) is similar to one found earlier [22] for Mn tetraarylporphyrins. The character of both dependencies indicates that for all studied Mn porphine-like complexes, the
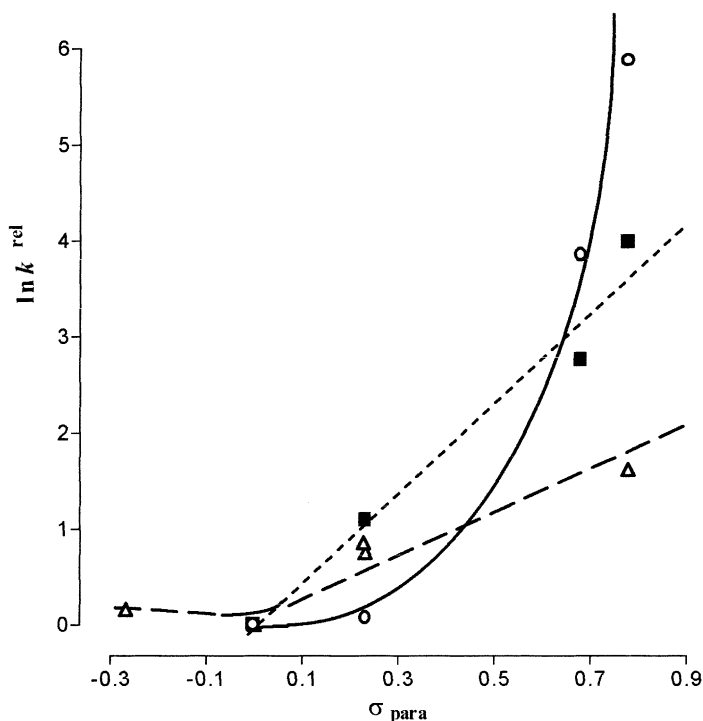
Fig. 9. The Hammett-type correlations of k_{ol}^{rel} ($\bigcirc$), k_1^{rel} ($\blacksquare$) for Mn(III) tetraazaporphines **1–4** and of k_{ol}^{rel} for RTDCPPMnCl ($\triangle$).

reaction of Mn-oxo-species formation is determined by both acceptor properties of Mn ion and donor ones of the macrocycle. It means that there is a *two-centered and two-component donor–acceptor bond*, which links catalyst and oxidant molecules in the species producing Mn(V)-oxo-complex; therefore, it cannot be the salt-like peracetate RTAPMnOOAc, and a molecular complex **A** should be considered as a precursor of Mn(V)-oxo-species.

One of the main characteristics of molecular complex **A** is the degree of electron density transfer from a molecule-donor to a molecule-acceptor. The increase of the last should lead to magnification of O–O bond polarization in the molecule of coordinated peracetic acid, thus facilitating Mn(V)-oxo-complex formation. As known, complete charge transfer in donor–acceptor complex should be followed by UV–VIS spectra changes. Interestingly, that in the course of olefin and naphthalene oxidation in the conditions, when the high excess of peracid with respect to the catalyst allows mainly the presence of

the associated form ($[\mathbf{A}] \cong [\text{catalyst}]_0$) and electronic spectra should be referred to **A**, the spectral changes of Mn(III) porphyrins and Mn(III) tetraazaporphines are different. Really, in the reaction of *cis*-stilbene epoxidation catalyzed by RTDCPPMnCl (R = H, NO_2), we have not observed spectral changes of Mn porphyrins in the visible region until full conversion of olefin (Fig. 10).[4] This indicates that electron transfer between Mn porphyrin and peracetic acid in the intermediate $\mathbf{A}^{Por}$ is not complete. If the same reaction is catalyzed by Mn tetraazaporphine **1**, its visible spectrum is drastically changed at the very beginning of the reaction (Fig. 11a); similar phenomena was also observed in naphthalene oxidation (Fig. 11b). The observed spectral changes can be explained by complete electron transfer from the tetraazaporphine macrocycle to the coordinated AcOOH molecule in

---

[4] TDCPPMnX oxidative degradation becomes noticeable *after* the exhaustive olefin oxidation (20 min in the conditions shown in Fig. 10).
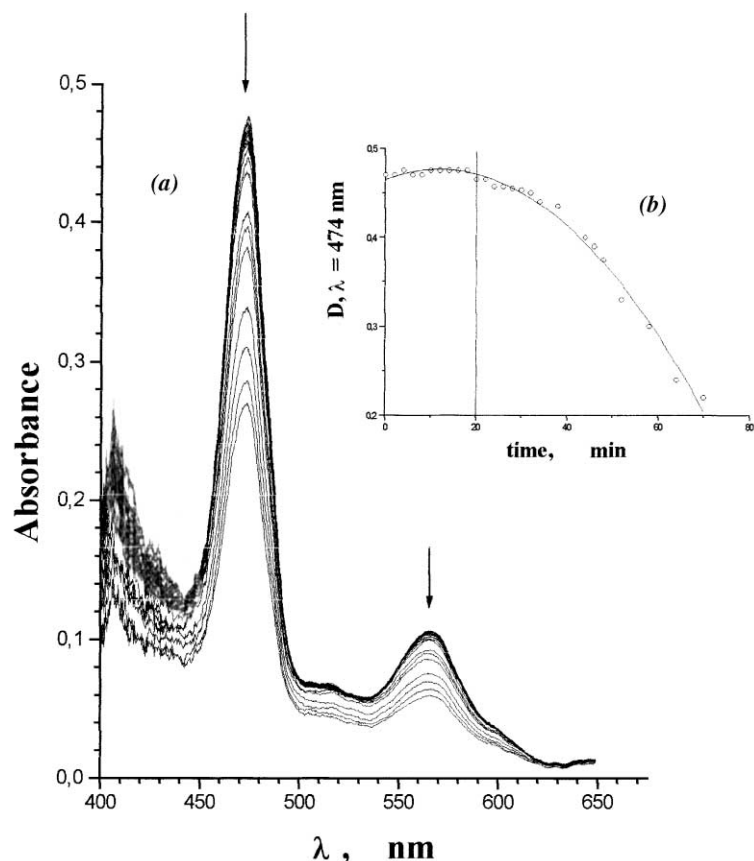
Fig. 10. (a) Visible spectra changes in the oxidation of *cis*-stilbene (0.01 M) by peracetic acid (0.05 M) catalyzed by Mn(III) meso-tetra(2,6-dichlirophenyl)porphyrin (1×10^{-5} M), $[AcOH]_{ox} = 0.5$ M, $l = 1$ cm; (b) monitoring of the reaction solution at $\lambda = 474$ nm (under the same conditions the total time of *cis*-stilbene exhaustive oxidation is 20 min).

the corresponding molecular complex ($\mathbf{A}^{TAP}$). Hence, we believe that $\mathbf{A}^{TAP}$ is a complex of Mn(III) porphyrazine π-cation radical with deeply polarized AcOOH molecule (Fig. 12). Indeed, one of the primary products of azaporphines oxidative degradation is known to be a product of nucleophilic addition to the C_{α}-pyrrole atom [39], thus confirming the localization of donor component **d**. If our explanation of these experimental observations is correct, the corresponding porphyrin's intermediate ($\mathbf{A}^{Por}$) should be more strong acids than $\mathbf{A}^{TAP}$. Really, the rate of PcZn bleaching in the Mn porphyrins-depending reaction was not changed at $[AcOH]_0 = 0.1$–0.4 M [22], whereas the RTAPMnCl-catalyzed reaction exhibits

such dependence (Fig. 8). According to Eq. (6), it means that $K_d^{Por} > K_d^{TAP}$. [5]

So, two lines of experiments are described by the same hypothesis, the key point of which is that coordinated peracetic acid is more strongly polarized being complexed with Mn tetraazaporphines than with Mn porphyrins, the former thus should be more active in Mn-oxo-moieties generation than the latter.

_____
[5] Slight variation of K_d on the substituent nature in Mn tetraazaporphines evidences that the degree of electron density transfer between Mn tetraazaporphine and coordinated peracetic acid is about not influenced by the substituent nature, possibly due to a mechanism of charge-transfer between Mn ion, tetraazaporphine macrocycle, and a molecule of coordinated peracid.
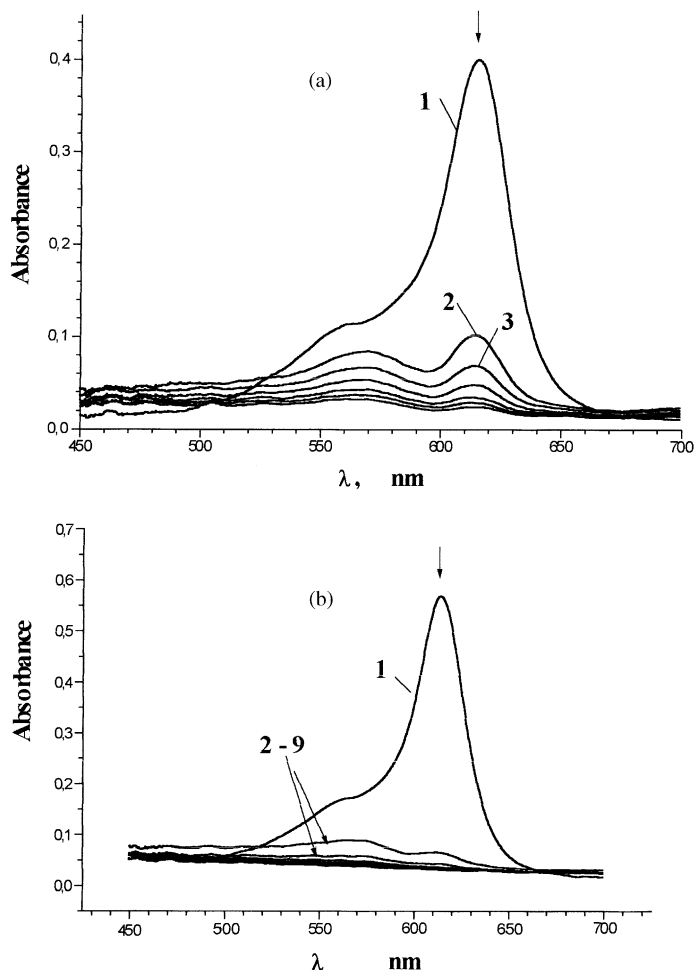
Fig. 11. Visible spectra changes in the oxidation of 0.01 M *cis*-stilbene (a) and 0.005 M naphthalene (b) by 0.05 M AcOOH catalyzed by complex **1** (1×10^{-5} M) at $[AcOH]_0 = 0.5$ M, $l = 1$ cm — (a) **1**: before AcOOH adding; **2**, **3** and further: spectra scanning every 5 s (under the same conditions the total time of *cis*-stilbene exhaustive oxidation is 5 min); (b) **1**: before AcOOH adding; **2**: after 5 s reaction; **3–9**: spectra scanning every 20 s (under the same conditions maximal naphthalene conversion is achieved at the reaction time of 8 min).

Really, for all Mn tetraazaporphines, especially for nitro-derivatives, k_2 values are higher than that ones for their porphyrins analogs (Tables 1 and 2). The more expressive Hammett-type correlation of k_2 for Mn tetraazaporphines could be explained by closer disposition of the substituent to the reaction center (Mn ion) in Mn tetraazaporphines (β-position of pyrrole ring) than in Mn meso-tetraarylporphyrins (*p*-position of phenyl ring). Recently, the enhanced reactivity in the epoxidation and hydroxylation reactions of Mn β-octafluoro-meso-tetra(2,6-dichlorophenyl)porphyrin

as compared with Mn meso-tetra(2,3,4,5,6-pentafluorophenyl)porphyrin has been demonstrated [40].

This explanation, though, is not suitable for the interpretation of different dependence of k_1 values on the substituent nature for the studied Mn porphine-like complexes. Indeed, whereas the values of k_1 for all Mn porphyrins are nearly identical (Table 2), the linear free energy relationships between $\ln k_1^{rel}$ with *positive* ρ value is observed for Mn tetraazaporphines (Table 3, Fig. 9). For Mn porphyrins, the independence of k_1 on the substituent nature was explained
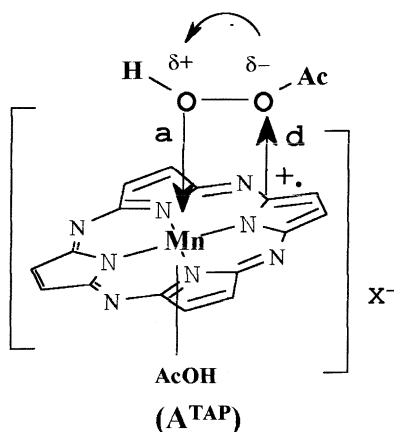
Fig. 12. The proposed structure of the intermediate $\mathbf{A}^{TAP}$ (the substituents in β-positions of pyrrole rings are omitted for the simplicity).

[22] by full compensation in energy of donor and acceptor components on the stage of donor–acceptor complex $\mathbf{A}^{Por}$ formation. This phenomena reveals the mechanism of electron density transfer from the periphery of the macrocycle to Mn(III) ion, experimentally observed for Mn(II) (and Mn(III)) phthalocyanines [41] and theoretically calculated for numerous porphine-like systems [42]. Similar K_2 values of the equilibrium RTAPMn(V)(O) $\leftrightarrow$ $^{\bullet +}$RTAPMn(IV)(O) calculated from Eqs. (2) and (3) for complexes **1**, **3**, and **4** (0.875, 1.33, 1.06) support this hypothesis.

For Mn porphyrazines, the growth of k_1 values at electronegative substitution evidences that acceptor properties of Mn(III) ion and donor ones of aza macrocycle vary in a significantly different degree at the peripheral substituent variation. This conclusion agrees with theoretical predictions. Really, all-electron ab initio Hartree–Fock self-consistent field calculations of the orbital energies of non-metallic porphine-like compounds [42] evidence that meso-tetraaza substitution in the porphyrine macrocycle results in a significant increase both in the first ionization potential of porphyrazine (tetraazaporphine) and in the core ionization potentials of the central nitrogen atoms. The last should give rise to a significantly higher oxidation potential of metal ion complexed to a porphyrazine than to an analogous porphyrin. Furthermore, the calculations revealed that the core

ionization potential of the central nitrogen is much more sensitive to electronegative substitution in a porphyrazine molecule than in a porphyrin one. It was concluded that electron-withdrawing peripheral substituents in porphyrazines should cause drastic shifts in the ionization potentials of the central nitrogens, which in turn results in an additional magnification of an oxidation potential of complexed metal ion. According to these predictions, acceptor properties of metal ion in Mn porphyrazines (especially in nitro-derivatives) should be increased in a dramatic fashion in comparison with the porphyrin analog both by meso-tetraaza substitution and by peripheral electron-withdrawing substituents. These theoretical predictions are in full agreement with the reported here k_1 dependence in Hammett's coordinates and with the considerably increased values of k_1 for nitro-substituted Mn tetraazaporphine as compared with analogous Mn porphyrin (2.7×10^5 and $2.3 \times 10^2 \, dm^3 \, mol^{-1} \, s^{-1}$ for **4** and NO_2TDCPPMnCl, respectively).

Whereas the first stage of peracetic acid interaction with Mn porphine-like complexes is determined by the ability of porphine-like molecule to bind peracid molecule, the efficiency of **A** transformation to Mn-oxo-complexes, as we have already mentioned, should depend on the degree of the coordinated O–O bond polarization. The last can be enhanced by both electron donation from a macrocycle to O–O bond and electron withdrawing from it by Mn ion. Thus, we believe that donor component **a** plays significant role in the second stage of the discussed reaction, giving rise to non-linear Hammett-type dependence of k_2 both for porphyrazine and porphyrin manganese complexes. The enhanced degree of O–O polarization (so $k_2 = k_{ol}$) in $\mathbf{A}^{TAP}$ at electronegative substitution should be considerably higher than in porphyrin analogs through both complete electron transfer along the donor component **a** and the extremely increased acceptor properties of Mn ion. Indeed, k_{ol} value for **4** is 250 times higher than for the corresponding Mn porphyrin (Tables 1 and 2). For H-substituted **1** or for complex **2** with the substituent of moderate strength (bromine), the acceptor properties of Mn ion, though enhanced by aza substitution, are not additionally affected by peripheral one. As a result, k_{ol} values of **1** and **2** slightly differ from those of their carbo-analogs (3.5 and 1.8 times, respectively; Tables 1 and 2).

4. Conclusions

Mechanism of peracetic acid interaction with Mn complexes of substituted tetra-R-tetra-*tert*-butyltetraazaporphines (R = H, Br, PhSO$_2$, NO$_2$) in acetonitrile/acetic acid solutions has been studied and compared with the established earlier for Mn-(III) meso-tetra(*o,o'*-dichloro-*p*-R-phenyl)porphyrins (R = MeO, H, Br, Cl, NO$_2$). The *trans*-stilbene, naphthalene, 1,1-diphenyl-2-picrylhydrazine, and tetra-4-*tert*-butyl-phthalocyanine zinc have been used as scavengers of high-reactive catalyst intermediates. In the presence of acetic acid excess, an acidic adduct [RTAPMn(AcOH)](X) interacts with peracetic acid via the formation of donor–acceptor complex **A** = [RTAPMn(AcOOH)(AcOH)](X) with complete electron transfer from tetraazaporphine macrocycle to the coordinated AcOOH molecule, donor and acceptor components being localized on the macrocycle and Mn ion, respectively. A linear Hammett-type dependence of the elementary rate constant of **A** formation k_1 with positive ρ value reveals the dominant role of acceptor properties of Mn ion on the first stage of the reaction.

The irreversible transformation of molecular complex **A** with elementary rate constant k_2 leads to the equilibrium mixture of Mn-oxo-species, supposedly RTAPMn(V)(O)(X) and $^{\bullet+}$RTAPMn(IV)(O)](X), the former epoxidizes olefins and the latter hydroxylizes naphthalene. For RTAPMnCl, the observed rate constant values of olefin epoxidation (k_{ol}) and naphthalene hydroxylation (k_{Nph}) are much more sensitive to the substituent nature than those ones for porphyrin analogs.

The experimentally determined rate constant $k_{ol} = k_2$ can be used as a criterion of Mn tetraazaporphines reactivity in Mn(V)-oxo-complex formation. Non-linear Hammett dependencies of $\ln k_{ol}^{rel}$ for both types of Mn porphine-like complexes revealed that donor properties of macrocycle so as acceptor ones of manganese ion play an important role in the formation of Mn(V)-oxo-moieties. This evidences that the latter are formed from a molecular complex **A** and that the corresponding peracetate, though exists, is not the precursor of the high-valent Mn-oxo-species.

Theoretically predicted significant enhancing of Mn ion electronegativeness by the electron-withdrawing substituents in the tetraazaporphine macrocycle could be the reason of the highest reactivity of nitro-substituted Mn porphyrazine in the studied reactions and in the aromatics oxidation to *p*-quinones as well [19].

Acknowledgements

References

[1] R.A. Sheldon (Ed.), Metalloporphyrins in Catalytic Oxidations, Marcel Dekker, New York, 1994.

[2] D. Mansuy, Coord. Chem. Rev. 125 (1993) 129.

[3] F. Montanari, L. Casella (Eds.), Metalloporphyrin Catalyzed Oxidation, Kluwer Academic Publishers, Dordrecht, 1994.

[4] J.T. Groves, J. Lee, S.S. Marla, J. Am. Chem. Soc. 119 (1997) 6269, and the references therein.

[5] T. Murakami, K. Yamaguchi, Y. Watanabe, I. Morishima, Bull. Chem. Soc. Jpn. 71 (1998) 1343, and the references therein.

[6] P.N. Balasubramanian, E.S. Schmidt, T.C. Bruice, J. Am. Chem. Soc. 109 (1987) 7865.

[7] T.G. Traylor, W.A. Lee, D.V. Stynes, J. Am. Chem. Soc. 106 (1984) 755.

[8] F. Minisci, F. Fontana, S. Araneo, F. Recupero, S. Banfi, S. Quici, J. Am. Chem. Soc. 117 (1995) 226.

[9] T.G. Traylor, C. Kim, J.L. Richard, F. Xu, C.L. Perrin, J. Am. Chem. Soc. 117 (1995) 3468.

[10] W.A. Lee, L.-C. Yuan, T.C. Bruice, J. Am. Chem. Soc. 110 (1988) 4277.

[11] L.-C. Yuan, T.C. Bruice, J. Am. Chem. Soc. 108 (1986) 1643.

[12] J.T. Groves, Y. Watanabe, J. Am. Chem. Soc. 110 (1988) 8443.

[13] O. Bortolini, M. Ricci, B. Meunier, P. Friant, I. Ascone, J. Goulon, New J. Chem. 10 (1986) 39.

[14] F. Montanari, M. Penso, S. Quici, P. Vigano, J. Org. Chem. 50 (1985) 4888.

[15] R. Song, A. Sorokin, J. Bernadou, B. Meunier, J. Org. Chem. 62 (1997) 673.

[16] W.-H. Wong, D. Ostovic, T.C. Bruice, J. Am. Chem. Soc. 109 (1987) 3428.

[17] S.V. Barkanova, O.L. Kaliya, J. Porph. Phthal. 3 (1999) 180.

[18] M. Filatov, N. Harris, S. Shaik, J. Chem. Soc., Perkin Trans. 2 (1999) 399.

[19] S.V. Barkanova, E.A. Makarova, O.L. Kaliya, E.A. Luk'yanets, Mendeleev Commun. 5 (1999) 177.

[20] S.V. Barkanova, I.A. Zheltukhin, O.L. Kaliya, V.N. Kopranenkov, E.A. Luk'yanets, Stud. Surf. Sci. Catal. (Dioxygen Act. Homogeneous Catal. Oxid.) 66 (1991) 471.

[21] A. Sorokin, B. Meunier, Chem. Eur. J. 2 (1996) 1308.

[22] S. Banfi, M. Cavazzini, G. Pozzi, S.V. Barkanova, O.L. Kaliya, J. Chem. Soc., Perkin Trans. 2 (2000) 871, 879.

[23] S. Banfi, F. Montanari, S. Quici, S.V. Barkanova, O.L. Kaliya, V.N. Kopranenkov, E.A. Luk'yanets, Tetrahedron Lett. 36 (1995) 2317.

[24] S. Banfi, M. Cavazzini, F. Coppa, S.V. Barkanova, O.L. Kaliya, J. Chem. Soc., Perkin Trans. 2 (1997) 1577.

[25] E.A. Makarova, V.N. Kopranenkov, V.K. Shevtsov, E.A. Lukyanets, Khim. Geterotsikl. Soedin. (Russ.) 327 (1994) 1206.

[26] L.P. Hammett, Physical Organic Chemistry, McGraw-Hill, New York, 1970.

[27] E. Gopinath, T.C. Bruice, J. Am. Chem. Soc. 113 (1991) 6090.

[28] O. Almarsson, T.C. Bruice, J. Am. Chem. Soc. 117 (1995) 4533.

[29] S. Banfi, F. Montanari, S. Quici, Recl. Trav. Chim. Pay-Bas 109 (1990) 117.

[30] S.-J. Zhu, M.-D. Gui, D.-X. Jiang, Chin. J. Chem. 13 (1995) 442.

[31] J.A. Smegal, C.L. Hill, J. Am. Chem. Soc. 105 (1983) 2920.

[32] J.A. Smegal, B.C. Schardt, C.L. Hill, J. Am. Chem. Soc. 105 (1983) 3510.

[33] J.T. Groves, Y. Watanabe, J. Am. Chem. Soc. 110 (1988) 8443.

[34] J.T. Groves, Y. Watanabe, T.J. McMurry, J. Am. Chem. Soc. 105 (1983) 4489.

[35] K. Yamaguchi, Y. Watanabe, I. Morishima, J. Am. Chem. Soc. 115 (1993) 4058.

[36] K. Machii, Y. Watanabe, I. Morishima, J. Am. Chem. Soc. 117 (1995) 6691.

[37] V.I. Gavrilov, L.G. Tomilova, I.V. Shelepin, E.A. Luk'yanets, Elektrokhim. Russ. 15 (1979) 1058.

[38] S. Wolowiec, L. Latos-Grazynski, Inorg. Chem. 37 (1998) 2984.

[39] C.J. Pedersen, J. Org. Chem. 22 (1957) 127.

[40] E. Porhiel, A. Bondon, J. Leroy, Eur. J. Inorg. Chem. (2000) 1097.

[41] O.V. Dolotova, N.I. Bundina, O.L. Kaliya, E.A. Luk'yanets, J. Porph. Phthal. 1 (1997) 355.

[42] A. Ghosh, P.G. Gassman, J. Almlöf, J. Am. Chem. Soc. 116 (1994) 1932.